

## A 121.4dB DR, -109.8dB THD+N Capacitively-Coupled Chopper Class-D Audio Amplifier

Zhang, Huajun; Berkhout, Marco; Makinwa, Kofi A.A.; Fan, Qinwen

**DOI**

[10.1109/ISSCC42614.2022.9731737](https://doi.org/10.1109/ISSCC42614.2022.9731737)

**Publication date**

2022

**Document Version**

Final published version

**Published in**

2022 IEEE International Solid- State Circuits Conference (ISSCC)

**Citation (APA)**

Zhang, H., Berkhout, M., Makinwa, K. A. A., & Fan, Q. (2022). A 121.4dB DR, -109.8dB THD+N Capacitively-Coupled Chopper Class-D Audio Amplifier. In L. C. Fujino (Ed.), *2022 IEEE International Solid-State Circuits Conference (ISSCC): Digest of technical papers* (pp. 484-486). Article 9731737 (Digest of Technical Papers - IEEE International Solid-State Circuits Conference; Vol. 2022-February). IEEE. <https://doi.org/10.1109/ISSCC42614.2022.9731737>

**Important note**

To cite this publication, please use the final published version (if applicable).  
Please check the document version above.

**Copyright**

Other than for strictly personal use, it is not permitted to download, forward or distribute the text or part of it, without the consent of the author(s) and/or copyright holder(s), unless the work is under an open content license such as Creative Commons.

**Takedown policy**

Please contact us and provide details if you believe this document breaches copyrights.  
We will remove access to the work immediately and investigate your claim.

***Green Open Access added to TU Delft Institutional Repository***

***'You share, we take care!' - Taverne project***

**<https://www.openaccess.nl/en/you-share-we-take-care>**

Otherwise as indicated in the copyright section: the publisher is the copyright holder of this work and the author uses the Dutch legislation to make this work public.

## 31.2 A 121.4dB DR, -109.8dB THD+N Capacitively-Coupled Chopper Class-D Audio Amplifier

Huajun Zhang<sup>1</sup>, Marco Berkhout<sup>2</sup>, Kofi A. A. Makinwa<sup>1</sup>, Qinwen Fan<sup>1</sup>

<sup>1</sup>Delft University of Technology, Delft, The Netherlands

<sup>2</sup>Goodix Technology, Nijmegen, The Netherlands

Class-D amplifiers (CDAs) are often used in audio applications due to their superior power efficiency. Due to the sensitivity of the human ear, a large dynamic range (DR) is desired, and audio DACs with up to 130dB DR are commercially available [1]. However, the DR of the CDAs they drive is typically much lower [2-4], mainly due to the thermal noise introduced by the input resistors of their resistive feedback networks. Reducing this resistance is difficult, as it reduces the CDA's input impedance and increases the required loop-filter capacitance. Alternatively, the CDA could be configured as a capacitively coupled chopper amplifier (CCCA), whose capacitive feedback network could then achieve low noise without reducing input impedance. However, the large PWM component present at its output would then saturate its input stage. By exploiting the inherent PWM filtering present in a feedback-after-LC architecture, this paper presents a capacitively coupled chopper CDA, resulting in significantly improved DR and THD+N. The prototype achieves 8μV<sub>RMS</sub> of integrated output noise (A-weighted), a 121.4dB DR, and -109.8dB THD+N while delivering a maximum of 15/26W into an 8/4Ω load with 93%/88% efficiency.

A simplified single-ended block diagram of the CDA is shown in Fig. 31.2.1 (top). It employs a feedback-after-LC architecture, in which LC-filter nonlinearity is suppressed by the loop gain. An inner feedback path consisting of a 1<sup>st</sup>-order LPF placed around the output stage compensates for LC filter phase-shift and ensures stability even in the presence of LC filter spread [3]. In this work, a capacitive feedback network ( $C_{IN}$  and  $C_{FB}$ ) is used to establish CDA gain ( $8\times$ ). The amplifier's input stage can then be configured as a CCCA, whose gain ( $C_{IN}/C_{GAIN}=16\times$ ) attenuates the noise of the loop filter by 24dB. Since the LC filter ( $L=3.3\mu H$ ,  $C=1\mu F$ ,  $f_c=88kHz$ ) suppresses most of the PWM content produced by the output stage around multiples of  $f_{PWM}=4.2MHz$ , the CCCA can handle the error signal ( $V_{IN}-V_{FB}/8$ ) in a linear fashion, as shown in Fig. 31.2.1 (bottom).

Chopping mitigates the mismatch in the capacitive feedback network that would otherwise limit the PSRR of the CDA. The LC filter suppresses intermodulation between the chopping ( $f_{CHOP}$ ) and PWM ( $f_{PWM}$ ) frequencies and their harmonics. Nevertheless, since chopping demodulates frequency content from even multiples of  $f_{CHOP}$  to baseband,  $f_{CHOP}$  ( $\approx 200kHz$ ) is set to an odd (21) sub-harmonic of  $f_{PWM}$  so that residual intermodulation products will occur around  $f_{CHOP}$  and its harmonics, thus far above the audio band [5]. Due to the non-linearity of the chopper switches and the CCCA's finite slew rate, chopping transitions will also cause nonlinear glitches, and thus distortion, at the CCCA's output. To maintain linearity, these glitches are blocked by a dead-band (DB) switch [5]. Its periodic time-varying action, however, will fold wideband noise from the CCCA,  $V_{IN}$ , and  $V_{FB}$  to the baseband. Therefore, the DB duration (25ns) is made only slightly longer than the CCCA's settling time. To ensure good tracking over PVT, the DB is generated by an RC delay, and the same type of resistor is used in the CCCA's constant- $g_m$  biasing circuit. All other timing signals, including  $f_{CHOP}$  and  $f_{PWM}$ , are derived from an on-chip RC oscillator (trimmed for 4.2MHz  $f_{PWM}$ ).

Figure 31.2.2 shows a schematic of the CCCA. It consists of a 2-stage Miller-compensated opamp in a capacitive feedback network. To mitigate  $1/f$  noise, the 1<sup>st</sup> stage of the CCCA is chopped. The CDA's input ( $V_{IN}$ ) and feedback ( $V_{FB}$ ) signals drive  $C_{IN}$  and  $C_{FB}$  via choppers  $CH_{IN}$  and  $CH_{FB}$ , respectively.  $C_{IN}$  (3pF) is chosen such that the parasitic capacitance at the virtual ground ( $V_X$ ) of the opamp does not significantly boost its input-referred noise. The DC level at  $V_X$  is set by a duty-cycled resistor  $R_{DC}$  (250MΩ) to be equal to the CCCA's output CM voltage (0.9V).

In contrast to most CCCA prior arts, which were intended for amplifying millivolt-level signals, the CCCA in this work must handle much larger (14.4V peak) signals from the CDA output via  $CH_{FB}$  and still ensure good linearity. As shown in Fig. 31.2.3,  $CH_{FB}$  is realized with back-to-back LDMOS devices. Level-shifters translate the chopping clock  $\Phi_{CH}$  from the low-voltage (LV, 1.8V) domain to the 14.4V domain, and their outputs are applied to switch drivers, which are powered by locally regulated bootstrap supplies ( $V_{REG1-4}$ ) derived from the output ( $V_{CP}$ ) of a shared on-chip charge pump to create an on- $V_{GS}$  of -4V [4]. The use of deadbanding blocks the signal-dependent delay of the level shifters ( $\sim 3ns$ ), which would otherwise lead to distortion.

Since both  $V_{IN}$  and  $V_{FB}$  can swing rail-to-rail, the timing skew ( $\Delta t$ ) between  $CH_{FB}$  and  $CH_{IN}$  clocks caused by the level shifters would cause voltage pulses of up to  $\sim 2V_{DD}$  at the virtual ground ( $V_X$ ) of the CCCA (Fig. 31.2.2), which would overstress its input devices. Moreover, larger glitches (up to several volts) could occur when  $CH_{FB}$  flips, in case  $R_{ON}$  of  $CH_{IN}$  ( $R_{ON,IN}$ ) is much higher than that of  $CH_{FB}$  ( $R_{ON,FB}$ ). Ideally,  $R_{ON,IN}$  should be  $\sim 8\times$  ( $=C_{IN}/C_{FB}$ ) lower than  $R_{ON,FB}$  to avoid these glitches. However, this is difficult because, in the chosen process, the LDMOS devices in  $CH_{FB}$  have a fixed length and can contribute significant  $1/f$  noise compared to their LV counterparts. Therefore, they are sized much wider for low  $1/f$  noise, resulting in a low  $R_{ON,FB}$  (11Ω). Although  $R_{ON,IN}$  could be sized accordingly to  $11\Omega/8$ , this would greatly increase the required area of the switches and their gate bootstrap capacitors (needed to make  $R_{ON}$  signal-independent for high linearity). Clamps could be used at  $V_X$  to restrict the pulses and glitches, but when activated, they inject charge into  $V_X$ , offsetting it by up to  $\sim V_{DD}$ , which would saturate the CCCA. To address the timing skew, as shown in Fig. 31.2.2, a level-shifter replica timing-skew-correction circuit is added to align the high-voltage (HV) and LV chopper clocks. To resolve large glitches due to the imbalance between  $R_{ON,IN}$  and  $R_{ON,HV}$ , a resistor  $R_{HV}$  is added in series with  $C_{FB}$ , which is set to 2.4kΩ ( $\sim 8\times R_{ON,IN}$ ) and has a negligible thermal and  $1/f$  noise contribution. The remaining glitches (due to the residual timing and impedance mismatch between the LV input and HV feedback paths) are kept well below  $V_{DD}$  ( $<900mV$  peak-to-peak differential) over PVT and are blocked by the DB switches.

Due to the large voltage excursions experienced by the  $CH_{FB}$  switches during chopping transitions, the switch drivers must be carefully designed to avoid cross-conduction. An example of such a transition is highlighted in Fig. 31.2.3, where some terminals of the  $CH_{FB}$  switches  $M_{1,3}$  experience large voltage excursions, whose  $dV/dt$  is set by the  $R_{ON}$  of the pull-up PMOS device ( $M_P$ ) used to drive  $M_1$  [6]. Parasitic coupling through the  $C_{GD}$  of  $M_3$  could then turn it on due to the IR drop across its pull-down NMOS ( $M_N$ ), thus creating a low impedance path between  $V_{FB+}$  and  $V_{FB-}$ . Due to parasitic inductance of the bond wires connecting  $CH_{FB}$  to the load, the resulting current pulses can cause significant ringing at nodes  $V_{FB+,INT}$  and  $V_{FB-,INT}$  (up to several volts, depending on driver design and  $L_{BOND}$ ), stressing the connected switches and their drivers, and exacerbating glitches at the virtual ground. To minimize such events, the  $R_{ON}$  of the NMOS pull-down transistors (e.g.,  $M_N$ ) must be made lower than that of their PMOS pull-up counterparts (e.g.,  $M_P$ ) by at least a factor of  $V_{REG}/V_{TH}$  [6]. In this work,  $R_{ON}$  of  $M_N$  is chosen to be  $7\times$  lower than that of  $M_P$  to ensure robustness across PVT.

Prototyped in a 180nm BCD process, the CDA occupies 7mm<sup>2</sup>, Fig. 31.2.7. Its audio performance is measured using an APx555 analyzer. Figure 31.2.4 (top) shows the measured FFT spectrum while the CDA delivers 1W into an 8Ω load, achieving a THD+N of -109.6dB. With a -80dBFS output, an SNR of 41.4dB is achieved, which corresponds to a DR of 121.4dB, Fig. 31.2.4 (bottom). The measured integrated output noise is 8μV<sub>RMS</sub> after A-weighting. Figure 31.2.5 (top) shows the measured THD+N across output power for 8Ω and 4Ω loads, resulting in a peak THD+N of -109.6dB and -109.8dB, respectively. As shown, the noise floor is 10dB lower than that obtained with a pair of 20kΩ input resistors, as are often used in resistive CDAs [2]. Figure 31.2.5 (bottom) shows the measured THD+N vs. input frequency. The CDA consumes a quiescent current of 9mA and can deliver a maximum of 15/26 W into an 8/4Ω load (measured at 10% THD) with a peak efficiency of 93%/88%. Figure 31.2.6 summarizes the performance of this work and compares it with state-of-the-art HV CDAs. Among the CDAs in Fig. 31.2.6, this is the only one to employ a capacitively-coupled chopper topology, with  $2.4\times$  lower integrated output noise, 5.9dB higher DR, 2.5dB better THD+N, and a competitive PSRR.

### References:

- [1] Cirrus Logic, *CS43131 130 dB, 32-Bit High-Performance DAC with Integrated Headphone Driver and Impedance Detection*, [Online]. Available: [https://statics.cirrus.com/pubs/proDatasheet/CS43130\\_F1.pdf](https://statics.cirrus.com/pubs/proDatasheet/CS43130_F1.pdf)
- [2] Texas Instruments, *TPA3255-Q1 315-W Stereo, 600-W Mono PurePath™ Ultra-HD Analog-Input*, [Online]. Available: <https://www.ti.com/lit/gpn/tpa3255-q1>
- [3] H. Zhang et al., "A -121.5 dB THD Class-D Audio Amplifier with 49 dB Suppression of LC Filter Non-linearity and Robust to  $\pm 30\%$  LC Filter Spread," *IEEE Symp. VLSI Circuits*, pp. 1-2, June 2021.
- [4] H. Zhang et al., "A -109.1 dB/THD/THD+N Chopper Class-D Amplifier with  $>83.7$  dB PSRR Over the Entire Audio Band," *ESSCIRC*, pp. 1-2, Sept. 2021.
- [5] H. Chandrakumar and D. Marković, "A 15.2-ENOB 5-kHz BW 4.5-μW Chopped CT  $\Delta\Sigma$ -ADC for Artifact-Tolerant Neural Recording Front Ends," *IEEE JSSC*, vol. 53, no. 12, pp. 3470-3483, Dec. 2018.
- [6] M. Berkhout, "A Class-D Output Stage with Zero Dead Time," *ISSCC*, pp. 134-135, Feb. 2003.

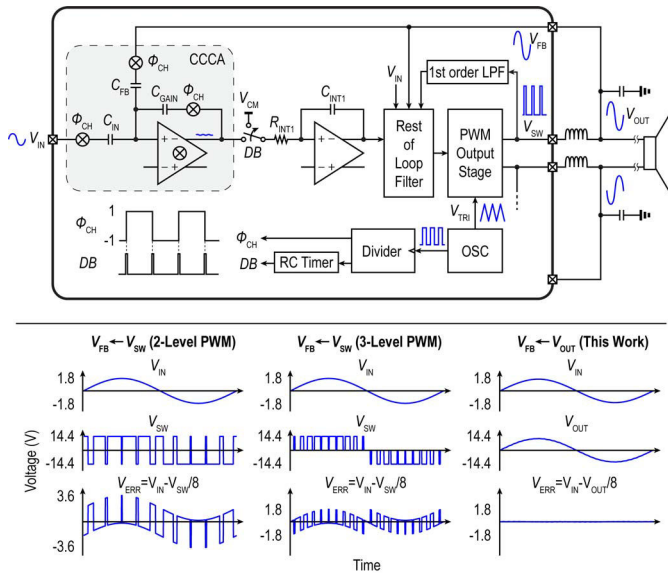


Figure 31.2.1: (Top) Architecture of the proposed capacitively-coupled chopper CDA, (bottom) error-signal waveform with  $V_{FB}$  taken from  $V_{SW}$  or  $V_{OUT}$ .

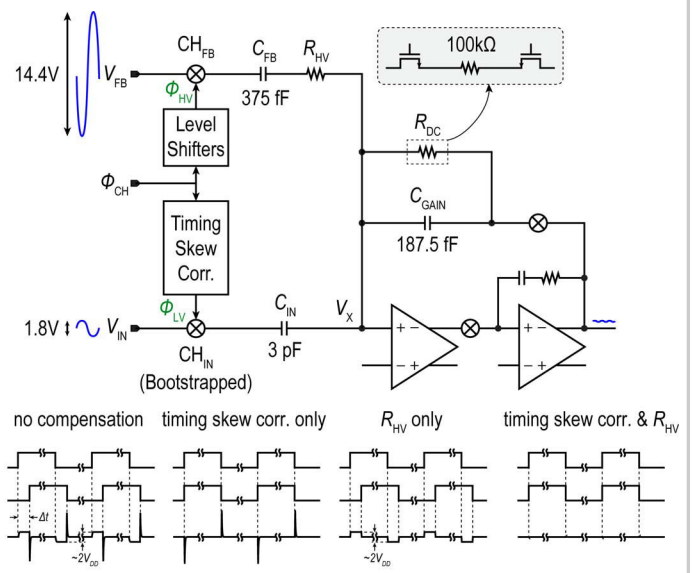


Figure 31.2.2: Schematic of the CCCA and the virtual-ground waveform with/without timing skew correction and/or impedance balancing ( $R_{HV}$ ).

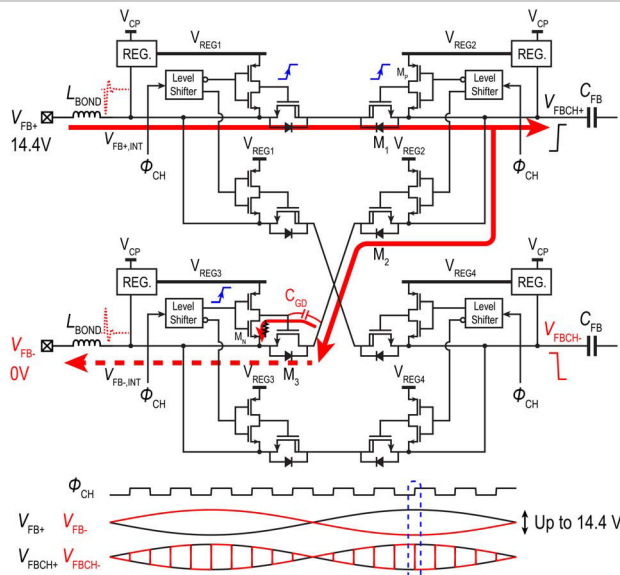


Figure 31.2.3: High-voltage chopper (CH\_FB) schematic and relevant transients during the highlighted chopping event.

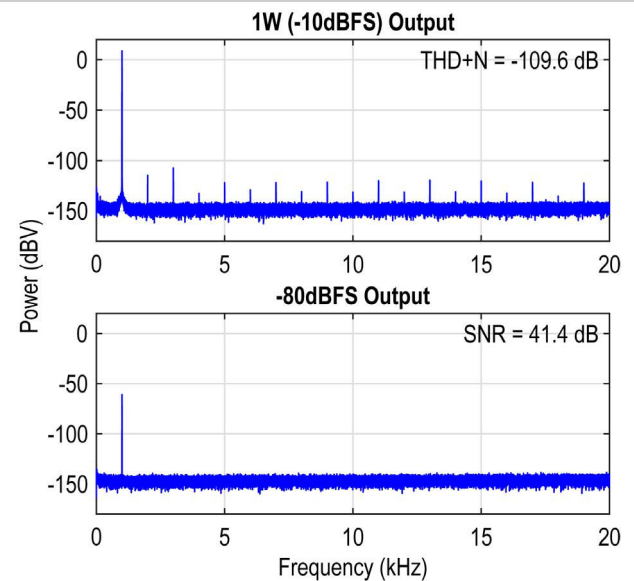


Figure 31.2.4: Measured output spectra when the CDA delivers (top) 1W (i.e., -10dBFS) and (bottom) -80dBFS to an 8Ω load.

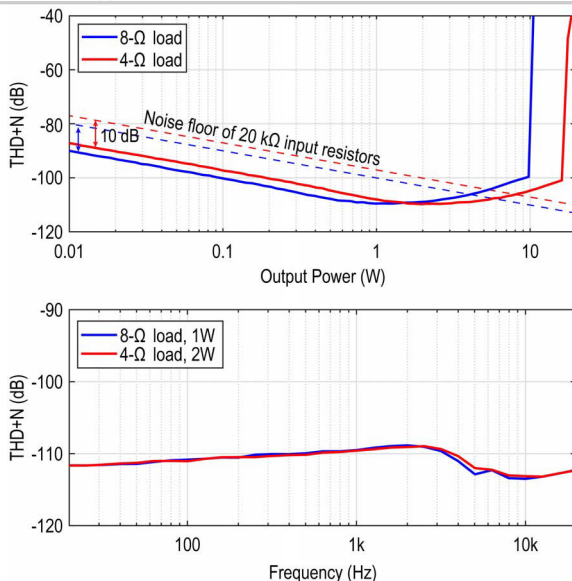
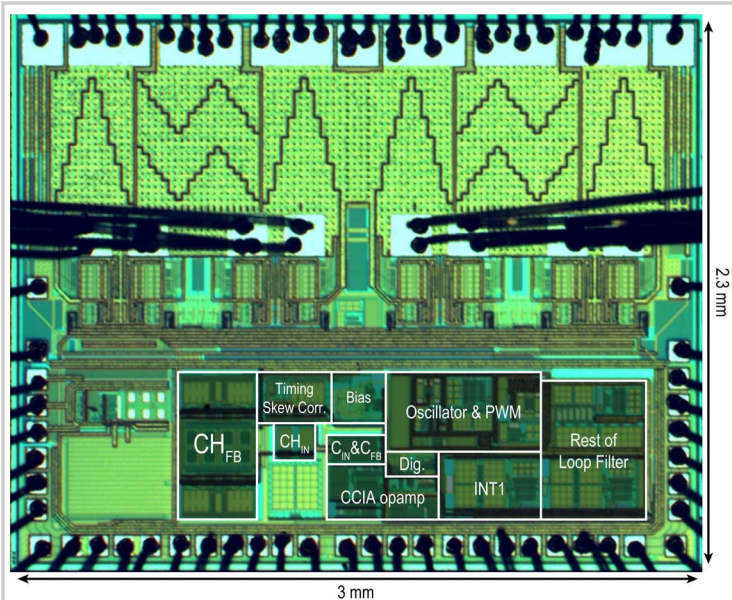


Figure 31.2.5: Measured THD+N (top) across output power for a 1kHz input and (bottom) across input frequency.

	This Work	TPA3255 [2]	Zhang VLSI'21	Karmakar ISSCC'20	Cope ISSCC'18	Schinkel JSSC'17
Process	180 nm BCD	-	180 nm BCD	180 nm BCD	180 nm BCD	130 nm BCD
Architecture	Analog-In	Analog-In	Analog-In	Analog-In	Digital-In	Digital-In
Feedback Network	Capacitive	Resistive	Resistive	Resistive	Resistive	Resistive
Supply (V)	14.4	51	14.4	14.4	8-20	14/25
Area (mm <sup>2</sup> )	7	-	6	4.8	4.3	-
$R_{LOAD}$ (Ω)	8/4	4	8/4	4	8	4
$P_{OUT,MAX}$ (W)	15/26	315	12/21	28	20	80
Efficiency	93%/88%	~90%**	91%/87%	91%	90%	>90%
$I_O$ / Channel (mA)	9	24	8	17	21	12
THD+N (dB)	-109.6/-109.8	-84	-107.1/-105.6	-102.2	-97.7	-88.6
DR	121.4	113	110*	109	115.5	115
A-wt. Output Noise ( $\mu V_{RMS}$ )	8	85	-	31	20	19/34
PSRR (dB) (Frequency/Hz)	89-71 (20-20k)	>65 dB	-	70-62 (20-20k)	80-50 (20-20k)	90-60** (20-20k)

\*SNR number used  
\*\*Estimated from graph

Figure 31.2.6: Performance summary and comparison to prior art.



**Figure 31.2.7: Die micrograph.**